

Disorders of the Nervous System

Synaptojanin1 Modifies Endolysosomal Parameters in Cultured Ventral Midbrain Neurons

Xinyu Zhu, Sanjana Surya Prakash, Geoffrey McAuliffe, and  Ping-Yue Pan<https://doi.org/10.1523/ENEURO.0426-22.2023>

Department of Neuroscience and Cell Biology, Robert Wood Johnson Medical School, Rutgers University, Piscataway, NJ 08854

Abstract

The accumulation of α -synuclein (α -syn)-enriched protein aggregates is thought to arise from dysfunction in degradation systems within the brain. Recently, missense mutations of *SYNJ1* encoding the SAC1 and 5'-phosphatase domains have been found in families with hereditary early-onset Parkinsonism. Previous studies showed that *Synj1* haploinsufficiency (*Synj1*^{+/-}) leads to accumulation of the autophagy substrate p62 and pathologic α -syn proteins in the midbrain (MB) and striatum of aged mice. In this study, we aim to investigate the neuronal degradation pathway using the *Synj1*^{+/-} MB culture from mouse pups of mixed sex as a model. Our data show that GFP-LC3 puncta formation and cumulative mKeima puncta formation are unaltered at baseline in *Synj1*^{+/-} MB neurons. However, GFP-LAMP1 puncta is reduced with a similar decrease in endogenous proteins, including lysosomal-associated membrane protein (LAMP)1, LAMP2, and LAMP2A. The LAMP1 vesicles are hyperacidified with enhanced enzymatic activity in *Synj1*^{+/-} MB neurons. Using a combination of light and electron microscopy (EM), we show that endolysosomal changes are primarily associated with a lack of SAC1 activity. Consistently, expressing the *SYNJ1* R258Q mutant in N2a cells reduces the lysosome number. Interestingly, the endolysosomal defects in *Synj1*^{+/-} neurons does not impact the clearance of exogenously expressed wild-type (WT) α -syn; however, the clearance of α -syn A53T was impaired in the axons of *Synj1*^{+/-} MB neurons. Taken together, our results suggest axonal vulnerability to endolysosomal defects in *Synj1*-deficient MB neurons.

Key words: α -synuclein; autophagy; lysosome; synaptojanin1

Significance Statement

The study by Zhu et al. discovered a previously uncharacterized role of *Synj1* in regulating endolysosomal number, protein, and acidity in ventral midbrain neurons. These alterations are associated with a specific impairment in the clearance of α -synuclein (α -syn) A53T, but not wild-type (WT) α -syn in axons, suggesting an essential role of *Synj1* in axonal degradative capacity under pathologic stress. This work in cultured mammalian neurons complements recent research efforts in *Drosophila*, *Caenorhabditis elegans*, and zebrafish and provides a novel insight for the role *Synj1* in neuronal degradation.

Introduction

Parkinson's disease (PD) is characterized by progressive loss of substantia nigra pars compacta (SNpc) dopamine (DA) neurons and the accumulation of Lewy bodies enriched in pathologic forms of α -synuclein (α -syn; Surmeier et al., 2017; Oliveira et al., 2021; Henderson et al., 2022).

While the exact cause of SNpc neuron loss remains elusive, bioinformatics analyses on familial inherited PD and sporadic PD have identified PD genes and risk loci that congregate in the autolysosomal pathway (Robak et al., 2017; Vázquez-Vélez and Zoghbi, 2021; Fleming et al., 2022; Udayar et al., 2022). Macroautophagy (hereafter

Received October 14, 2022; accepted March 28, 2023; First published April 18, 2023.

The authors declare no competing financial interests.

Author contributions: X.Z. and P.-Y.P. designed research; X.Z. and G.M. performed research; S.S.P. contributed unpublished reagents/analytic tools; X.Z. analyzed data; X.Z. and P.-Y.P. wrote the paper.

referred to as “autophagy” in this study) is a “self-eating” process that degrades a wide range of cytosolic components including misfolded proteins and damaged organelles to maintain cellular homeostasis (Klionsky, 2007; Nixon, 2013). This process involves the formation of mature autophagosomes followed by fusion with endolysosomes for degradation of cytosolic contents. Chaperone-mediated autophagy (CMA) is mediated by lysosomal-associated membrane protein (LAMP)2A-assisted protein translocation (Kon and Cuervo, 2010; Kaushik and Cuervo, 2018). It is less common but highly important for degradation of α -syn (Cuervo et al., 2004). Whether and how each individual PD gene is implicated in the autophagosome/lysosome dysfunction during pathogenesis remains to be elucidated.

Recently, missense mutations including R258Q, R459P and R839C in PARK20/SYNJ1 have been discovered in families with early onset parkinsonism (Krebs et al., 2013; Quadri et al., 2013; Kirola et al., 2016; Taghavi et al., 2018). Reduced SYNJ1 transcripts were also reported in a subset of sporadic PD brains (Pan et al., 2020). SYNJ1 encodes synaptojanin1/Synj1, a phosphoinositol phosphatase with two enzymatic domains: a 5'-phosphatase domain that specifically hydrolyzes the 5'-phosphate from the inositol ring of PI(4,5)P₂ (Guo et al., 1999; Pirruccello and De Camilli, 2012) and a SAC1-like domain that dephosphorylates PI3P, PI4P, and PI(3,5)P₂ into PI (Zhong et al., 2012). Interestingly, Synj1 was initially characterized to cooperate with endophilin to regulate synaptic vesicle recycling through regulating plasma membrane PI(4,5)P₂ levels and nascent clathrin coated vesicles (McPherson et al., 1996; Cremona et al., 1999; Verstreken et al., 2002, 2003). Since the identification of SYNJ1 mutations in PD, new investigations have emerged that examined the roles of Synj1 in the autolysosomal pathway. Recent studies in *Drosophila* and *Caenorhabditis elegans* showed that the SAC1 domain is required for autophagosome formation. The R258Q mutation, which abolishes SAC1 enzymatic activity, delays autophagosome maturation because of an accumulation of PI(3)P and PI(3,5)P₂ and/or disrupted Atg9 activity (Vanhouwaert et al., 2017; Yang et al., 2022). In cultured mouse cortical astrocytes, however, an increase in autophagosome formation was observed in cells from the Synj1-deficient background (Pan et al., 2021). Autophagy impairment was found in the later stages of autolysosomal degradation, and both phosphatase domains were involved in stress-induced clearance of p62 (Pan et al.,

2021). Consistently, in aged *Synj1* haploinsufficient (*Synj1*^{+/-}) mice an accumulation of the autophagy substrate p62 was observed in all brain regions including DA neurons in the midbrain (Pan et al., 2020). Additionally, in the cone photoreceptors of zebrafish retina, *Synj1* deletion led to mislocalization and abnormal accumulation of late endosomes and autophagosomes (George et al., 2014, 2016). While these recent studies present evidence for a novel role of *Synj1* in regulating the autophagic and autolysosomal functions, results obtained from different model systems are somewhat conflicting.

SYNJ1 downregulation was identified in a subset of sporadic PD patients (Pan et al., 2020), and we therefore decided to investigate *Synj1* heterozygous (*Synj1*^{+/-}) deficiency, which represents a more prevalent genetic condition than homozygous point mutations found in few families so far. In this study, we used multiple optical tools to analyze autophagosome and endolysosome structures in cultured *Synj1*^{+/-} midbrain neurons. We found that *Synj1* haploinsufficiency did not affect the basal level LC3-mediated autophagy flux in the soma of ventral MB neurons. Robust reduction was observed for the GFP-LAMP1 puncta number, endogenous LAMP1, LAMP2 and LAMP2a proteins, accompanied by endolysosomal hyperacidification. Further, we found the endolysosomal defect is associated with a reduction in SAC1 activity rather than 5'-phosphatase activity. More interestingly, the degradation of α -syn A53T, but not WT α -syn, was significantly impaired in the axons of *Synj1*^{+/-} neurons. Taken together, our results indicate specific vulnerability in axonal degradation in response to *Synj1* deficiency associated with endolysosomal dysfunction.

Materials and Methods

Plasmids, antibodies, and reagents

The following plasmids, pEGFP-C1-GFP-Synj1 WT, pEGFP-C1-GFP-Synj1 R258Q, pEGFP-C1-GFP-Synj1 R839C, pEGFP-C1-GFP-Synj1 D769A, pEGFP-C1-GFP-LC3 were previously reported (Pan et al., 2020, 2021). mKeima was gifted by Atsushi Miyawaki (Osaka University). The plasmid expressing LAMP1-GFP is a gift from Prof. Tao Xu (Institute of biophysics, Chinese Academy of Sciences). The FIRE-pHLy plasmid was purchased from Addgene (catalog #170775). Mouse WT or A53T α -syn cDNAs (gifted by Eliezer Masliah, National Institute on Aging) was cloned into pmEos3.2-N1 vector (from Addgene, catalog #54525) to generate the α -syn-mEos3.2/ α -syn A53T-mEos3.2 plasmid.

The GlutaMAX Supplement (35050061), the Neurobasal-A Medium (12349015), the B-27 Supplement (17504044), the basal medium Eagle (BME; 21010046), the DMEM (11965-092), the penicillin-streptomycin (15140122), the Lipofectamine 2000 Reagent (11668019), the Lipofectamine 3000 Transfection Reagent (L3000150), the DQ Red BSA (D12051), the LAMP-2A Polyclonal Antibody (51-2200, 1:100 for IF), the LAMP2 Polyclonal Antibody (PA1-655, 1:200 for IF), the LAMP-1 Monoclonal Antibody (14-1071-85, 1:500 for IF), the MAP2 Monoclonal Antibody (MAP2 MA5-12826, 1:1000 for IF), and all of the Alexa Fluor dye-

This work was supported by the National Institute of Neurological Disorders and Stroke Grant R01 NS112390 (to P.-Y.P.).

Acknowledgments: We thank Dr. Qian Cai for sharing the Cathepsin B antibody and Jessica Lee, Ariana Capuano, and Asma Rizvi for performing mouse breeding and genotyping to support this study. We also thank Jacqueline Saenz, Hana Caiola, and Mikayla Voglewede for critical reading of this manuscript.

Correspondence should be addressed to Ping-Yue Pan at pingyue.pan@rutgers.edu.

<https://doi.org/10.1523/ENEURO.0426-22.2023>

Copyright © 2023 Zhu et al.

This is an open-access article distributed under the terms of the Creative Commons Attribution 4.0 International license, which permits unrestricted use, distribution and reproduction in any medium provided that the original work is properly attributed.

conjugated secondary antibodies were purchased from Thermo Scientific. The Magic Red Cathepsin-B Assay kit (MR; 937) was purchased from Immunochemistry. The mouse Cathepsin B Antibody (AF965; 1:200 for IF) was purchased from R&D Systems, Inc. The anti-MAP2 Polyclonal Chicken Antibody (188006, 1:1000 for IF) and the anti-MAP2 Polyclonal Guinea Pig Antibody (188004, 1:1000 for IF) were purchased from Synaptic Systems. The anti-Tyrosine Hydroxylase Antibody (AB9702, 1:1000 for IF) was purchased from Millipore Sigma. The papain (LK003176) and the Earle's balanced salt solution (EBSS; LK003188) were purchased from Worthington Biochemical Corporation. The fetal bovine serum (FBS; S11510H) was purchased from Novus Biologicals.

Cell sorting and EM analysis

The N2a cells transfected with GFP-Synj1 WT or GFP-Synj1 R258Q on day 1 were sorted to collect GFP expressing cells by an fluorescence-activated cell sorting (FACS) equipment on day 2. Then, on day 4, the cells were fixed in the culture dish by replacing the culture medium with 2.5% glutaraldehyde in 0.1 M sodium cacodylate buffer containing 2.5 mM Ca^{2+} at room temperature (RT). After fixation for 60–90 min, the cells were rinsed three times with the same buffer, and then postfixed for 60 min with 1% osmium in the rinsing buffer containing 1% potassium ferricyanide. The cells were rinsed again with rinsing buffer and stained with 1% uranyl acetate at 4°C for 30 min. Dehydration with graded ethanol solutions was followed by infiltration and embedding with PolyBed812. After polymerization portions of the embedment were cut out and re-embedded in Polybed812. So, the cells could be sectioned perpendicular to the dish surface. Thin sections were viewed in a Philips CM12 electron microscope (EM) to capture images.

The diameter of lysosome was measured by drawing a line manually with the tool Straight Line in Fiji. To measure the density of lysosome, lysosome number was counted and divided by the entire cytoplasmic area defined in ImageJ.

Animal

The *Synj1*^{+/-} mice were originally from the Pietro De Camilli laboratory at Yale University (Cremona et al., 1999). They were housed and handled in accordance with the National Institutes of Health guidelines approved by the Institutional Animal Care and Use Committee. Approved IACUC protocol: PROTO201800183. C57bl/6 mice (Jax catalog #000664) and *Synj1*^{+/-} mice were used as breeders to generate *Synj1*^{+/+} and *Synj1*^{+/-} pups identified by genotyping. Both male and female pups were used for cell culture.

Immunofluorescence (IF)

The immunostaining protocol was previously described (Zhu et al., 2018; Pan et al., 2020) with minor modifications. Briefly, the cells were fixed with 4% PFA for 15 min at room temperature (RT), permeabilized with 0.5% saponin for 15 min at RT, blocking with 5% BSA for 1 h at RT, incubated with primary antibody overnight and incubated

with fluorescent dye conjugated secondary antibody for 1 h at RT. After complete washing with PBS, the slides were mounted with Clear-Mount (EMS, 17985-12).

MR and BSA-DQ analysis in MB culture

For MR staining, the MB culture was incubated with MR at 1:100 dilution in culture medium for 1 h, then the culture was subjected to live cell confocal imaging. For BSA-DQ staining, the MB culture was incubated with BSA-DQ (40 µg/ml diluted in culture medium) for 6 h, then the culture was subjected to live cell imaging. Glial cells expressing GFP were used as reference to record the stage locations of the imaged cells, whose neuronal identification was confirmed by MAP2 immunoreactivity during *post hoc* analysis guided by the stage location.

Midbrain culture preparation and transfection

The preparation of mouse ventral midbrain culture was described before (Pan et al., 2017, 2020). Briefly, after genotyping, the ventral midbrain tissue was dissected from postnatal day 0–1 littermates, and it was digested in a papain solution (21 U/ml, prepared with EBSS supplemented with 5 mM kynurenic acid) by stirring with a magnetic stir bar at 33–37°C for 12 min under humidified oxygenation. After spinning and discarding the digestion buffer, the collected tissue chunk was triturated by using a 1 ml pipette tip in Neuro A complete medium (0.6× Neurobasal-A Medium, 0.3× BME, 1× GlutaMAX Supplement, 1× B-27 Supplement, and 10% FBS). The homogenized tissue was collected by spinning and the supernatant containing debris was discarded. The pellet was resuspended with Neuro A complete medium and subjected for spinning again. Then, the supernatant was discarded, and the pellet was resuspended with Neuro A complete medium. After counting, 25,000 cells were seeded into a 6 × 8 mm cylinder. On day 3, medium was changed with fresh Neuro A complete medium with Ara-C (0.2 µM) to inhibit glia growth. Transfection was performed on days 3–5 using calcium phosphate solution, or on days 6–8 using Lipofectamine 2000 reagent or Lipofectamine 3000 Reagent. In either case, 0.7 µg DNA was transfected for each 6 × 8 mm area of culture.

N2a cell culture and transfection

N2a cells are cultured in 10% FBS contained DMEM medium supplemented with 10 U/ml penicillin-streptomycin. Passage procedure follows the general and standard culture protocol with digestion using 0.05% Trypsin-EDTA solution. Lipofectamine 2000 or Lipofectamine 3000 was used for plasmid transfection in N2a cells.

Imaging and data analysis

All fluorescent images were captured using a Nikon CREST spinning disk confocal microscope with a 100×, 60×, or 40× oil objective. And all the image analysis was performed by ImageJ/Fiji. For analyzing the immunofluorescence of LAMP1, LAMP2A, LAMP2, and Magic Red in neuron soma of glia-neuron culture, the floated neurons were selected for imaging. To further avoid the immunofluorescence contamination from

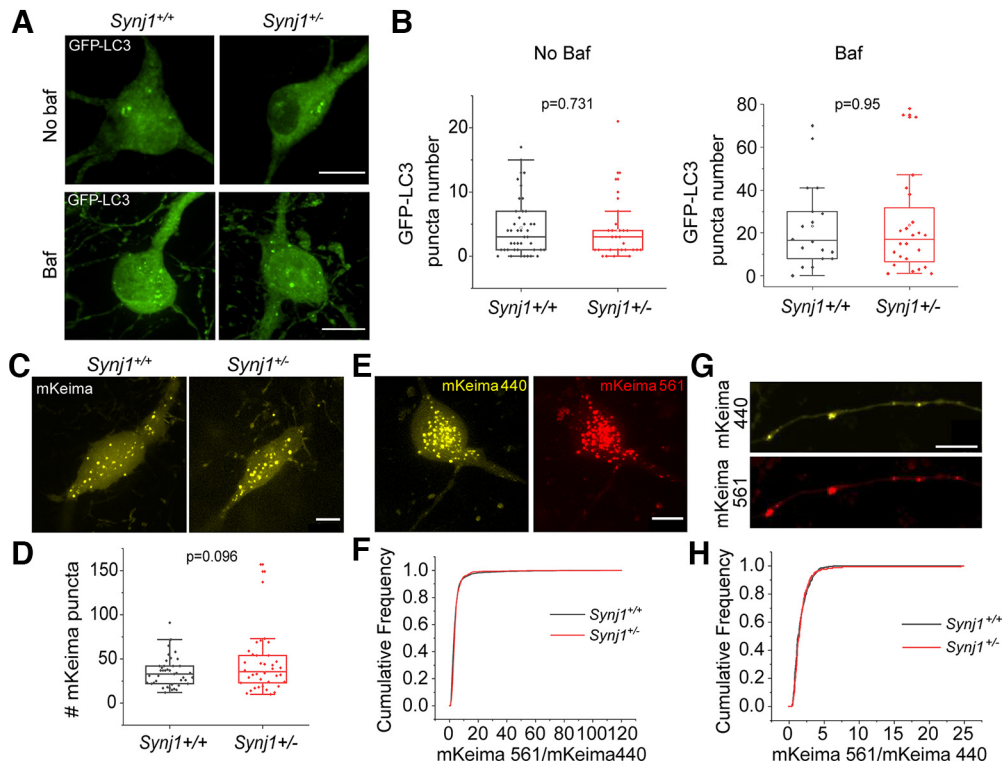


Figure 1. Synj1 deficiency does not substantially alter baseline autophagosome formation and flux in cultured MB neurons. **A, B**, GFP-LC3-labeled autophagosome in the soma of *Synj1*^{+/+} and *Synj1*^{+/-} MB neurons treated with/without 25 nM bafilomycin A1 for 6 h. **A**, Representative images. **B**, Quantification for the GFP-LC3 numbers at the soma. For no baf group, $N = 44/29$ (*Synj1*^{+/+}/*Synj1*^{+/-}) neurons, for baf group, $N = 18/24$ (*Synj1*^{+/+}/*Synj1*^{+/-}) neurons. **C, D**, mKeima-labeled autophagosome in the soma of *Synj1*^{+/+} and *Synj1*^{+/-} MB neurons. **C**, Representative images. **D**, Quantification for the mKeima puncta numbers at the soma, $N = 41/38$ (*Synj1*^{+/+}/*Synj1*^{+/-}) neurons. **E**, Representative images show mKeima signal in the soma of MB neuron following activation by 440- and 561-nm light. **F**, Distribution analysis of the ratio (mKeima561/mKeima440) for the mKeima puncta between *Synj1*^{+/+} and *Synj1*^{+/-} MB neurons, $N = 2355/899$ (*Synj1*^{+/+}/*Synj1*^{+/-}) puncta. **G**, Representative images show mKeima signal in the axon of MB neuron from activation by 440 and 561 nm. **H**, Distribution analysis of the ratio (mKeima561/mKeima440) for the mKeima puncta between *Synj1*^{+/+} and *Synj1*^{+/-} MB axons, $N = 297/177$ (*Synj1*^{+/+}/*Synj1*^{+/-}) puncta. The p values are from Student's t test. Scale bar in all images: 10 μ m.

glia, the upper confocal planes, no longer including fluorescent signal of glia, were selected for a Z-Max-Project performance. Then the cytoplasmic area of each neuron in the Z-MAX-Project image was circled to obtain the average value. For monitoring the fluorescent intensity of WT or A53T α -syn-mEos3.2 in neuron soma, the cytoplasmic area was circled after a Z-Max-Project performance to get the mean value. For ratiometric analysis of the puncta of mKeima and FIRE-pHly as well as the immunofluorescence (IF) of LAMP1, the plugin Time series Analyzer 3.2 was used to set ROIs defined as $0.66 \times 0.66 \mu\text{m}$ (six \times six pixels) at the soma or axons. For analyzing the LAMP1-GFP puncta at the axons, the plugin KymoAnalyzer V1.01 (Neumann et al., 2017) was employed to measure the puncta density. For analyzing the fluorescent intensity of α -syn/a-syn A53T at axons, the tool Segmented Line [width: $0.33 \mu\text{m}$ (three pixels)] is used to obtain the average value through tracing the axons.

Results

Synj1^{+/-} MB neurons exhibit normal autophagosome numbers and acidity at the basal level

Prior research has shown that in the brains of aged (12-month) male *Synj1*^{+/-} mice, p62 is increased in the cortex,

striatum, and MB DA neurons; however, enhanced LC3B level was only observed in the cortex and striatum but not in the MB DA neurons (Pan et al., 2020). To further investigate whether Synj1 regulates autophagy in MB neurons, we first transfected GFP-LC3 in cultured MB neurons from littermate *Synj1*^{+/+} and *Synj1*^{+/-} mice. All analyses were performed in mature neurons between days *in vitro* (DIV)13 and DIV16. Bafilomycin (Baf; 25 nM) was applied to the culture for 6 h to reveal the basal level autophagy flux. In both MB cultures treated with vehicle or baf, we found similar numbers of GFP-LC3 puncta in the cell bodies between *Synj1*^{+/+} and *Synj1*^{+/-} MB neurons (Fig. 1A,B), suggesting normal basal autophagy flux. GFP-LC3 puncta in the axons could not be determined with confidence in either *Synj1*^{+/+} or *Synj1*^{+/-} neurons and were therefore not included in the analysis. We next employed another molecular probe, mKeima, a pH-sensitive ratiometric fluorescent protein that is resistant to the lysosomal acidic environments. The mKeima is a cytosolic protein and mKeima puncta have been used as a measure of cumulative autophagic activity (Katayama et al., 2011). Less acidic (pH6–pH7) autophagosomes exhibit strong emission at 440-nm excitation but weak emission at 561-nm excitation, while more acidic autolysosomes (pH4–pH6) exhibit reverted emission ratio. No

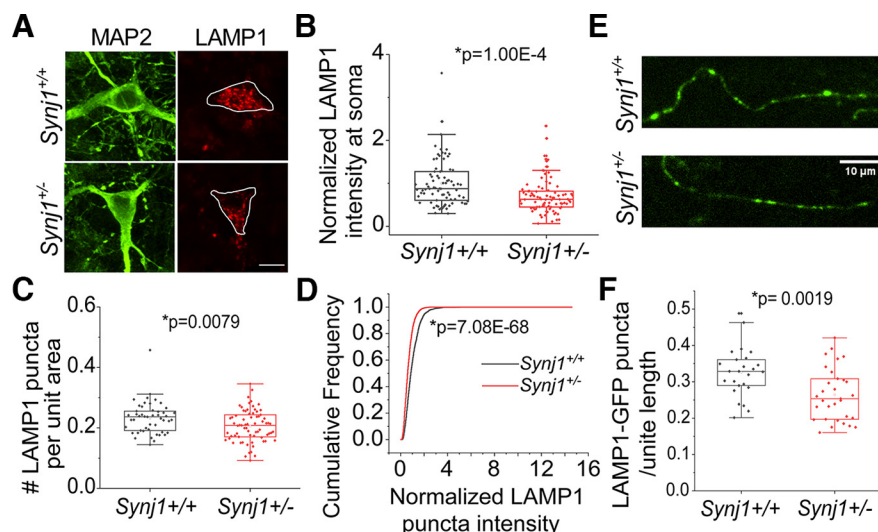


Figure 2. Reduced LAMP1 expression and puncta number in *Synj1*-deficient MB neurons. **A, B**, Immunofluorescence analysis of LAMP1 in the soma of *Synj1*^{+/+} and *Synj1*^{+/-} MB neurons, MAP2 is used as neuronal marker. **A**, Representative images. **B**, Quantification results, $N = 82/88$ (*Synj1*^{+/+}/*Synj1*^{+/-}) neurons. Extended Data Figure 2-1 shows reduced LAMP2 and LAMP2A in the soma of *Synj1*-deficient MB neurons. **C**, Quantification of LAMP1-labeled puncta for *Synj1*^{+/+} and *Synj1*^{+/-} MB neurons. y -axis represents the normalized puncta number per unit cytoplasmic area, $N = 82/88$ (*Synj1*^{+/+}/*Synj1*^{+/-}) neurons. **D**, Cumulative frequency graph shows the LAMP1 fluorescence intensity distribution of the puncta in soma between *Synj1*^{+/+} and *Synj1*^{+/-} MB neuron. $N = 2091/2873$ (*Synj1*^{+/+}/*Synj1*^{+/-}) puncta. **E, F**, Analysis of LAMP1-GFP puncta in the axons of *Synj1*^{+/+} and *Synj1*^{+/-} MB neurons. **E**, Representative images. **F**, Quantification results, $N = 25/31$ (*Synj1*^{+/+}/*Synj1*^{+/-}) axons. The p values for **B**, **C**, and **F** are from Student's t test. The p value for **D** is from two-sample Kolmogorov-Smirnov test. Scale bar in all images: 10 μm . Extended Data Figure 2-2 shows the comparison of LAMP1/LAMP2A expression between TH⁺ and TH⁻ MB neurons.

significant change in the mKeima puncta was observed in the *Synj1*^{+/-} neuronal soma overtime (within 7 d from transfection to imaging) compared with the *Synj1*^{+/+} neurons (Fig. 1C,D). Compared with GFP-LC3, mKeima was able to reveal a few more punctate structures along the axons (Fig. 1G); however, overall, these puncta were extremely sparse to justify an accurate analysis for axonal density. Thus, we only compared the acidity of mKeima structures by calculating the ratio of emissions at 440- and 561-nm excitations (Fig. 1E-H). We found that *Synj1* deficiency did not change the acidity of mKeima structures either at the soma (Fig. 1F) or the axons (Fig. 1G,H) of MB neurons. Therefore, by expressing GFP-LC3 and mKeima in cultured MB neuron, we were unable to identify a significant contribution of *Synj1* to autophagosome number and acidity at neuronal soma at the basal level.

Synj1 deficiency is associated with changes in the lysosomal-associated membrane proteins (LAMPs) in cultured MB neurons

We next investigated the endolysosomal system by examining endogenous expression of lysosome-associated proteins, including LAMP1, LAMP2, and LAMP2A. We found that in the soma of *Synj1*^{+/-} MB neurons the expression of LAMP1 was reduced by $\sim 25\%$ (Fig. 2A,B). Additionally, the density of LAMP1 structures was significantly lower (Fig. 2C), accompanying a reduction in the immunofluorescence of each LAMP1 puncta in *Synj1*^{+/-} MB neurons (Fig. 2D), suggesting a possible reduction of lysosome number and protein expression. Recent studies suggested that LAMP1 is not a reliable marker for lysosomes

because of its presence on late endosomes (Cheng et al., 2018a, b). We thus performed immunofluorescence for two additional LAMP proteins: LAMP2 and LAMP2A. LAMP2A is a specific isoform of LAMP2 that regulates chaperone-mediated autophagy (CMA; Cuervo and Dice, 1996; Cuervo et al., 2004). Consistently, we found a near 25% reduction in both LAMP2 (Extended Data Fig. 2-1A,B) and LAMP2A (Extended Data Fig. 2-1C,D) at the cell bodies of *Synj1*^{+/-} MB neurons. In both TH⁺ and TH⁻ neurons from the midbrain, similar reductions of lysosomal associated proteins were observed (Extended Data Fig. 2-2). The differences among TH⁺ neurons were less significant likely because of a smaller sample size. Nevertheless, our results suggest *Synj1* deficiency reduces the levels of LAMPs in ventral MB neurons. Because of the enriched expression of *Synj1* in the axons and synapses, we next sought to examine whether *Synj1* deficiency affects axonal lysosomal associated proteins. Using immunofluorescence, it was technically challenging to analyze these proteins at the axons in the mixed neuron-glia culture. We therefore expressed LAMP1-GFP in cultured MB neurons. Similarly, we found that the LAMP1 puncta density in the axons were significantly reduced in *Synj1*^{+/-} MB neurons (Fig. 2E,F). Together, these results suggest a previously unknown role of *Synj1* in regulating lysosomal associated proteins.

Hyperacidification of LAMP1 vesicles and increased protease activity in *Synj1*-deficient MB neurons

We next sought to determine whether function of the degradational vesicles, such as acidification and enzymatic activity, is impaired in *Synj1*-deficient MB neurons.

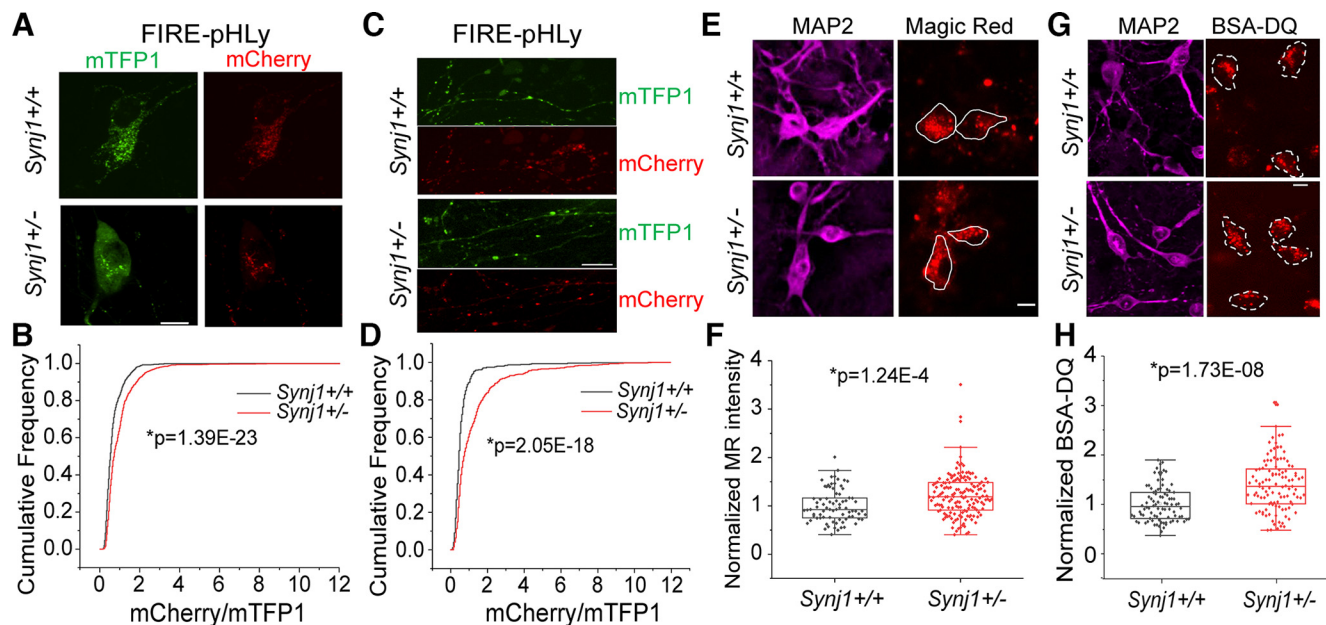


Figure 3. Synj1 deficiency leads to endolysosomal hyperacidification and enhanced enzymatic activity. **A–D**, Endolysosomal acidity assay using a ratiometric fluorescent probe pHLy. **A, C**, representative images showing the mTFP1 signal and mCherry signal in the soma (**A**) and axons (**C**) of MB neurons transfected with pHLy. The brightness and contrast were adjusted to the same range for mTFP1 and mCherry channels. **B, D**, Distribution analysis of the ratio (mCherry/mTFP1) for the pHLy-labeled puncta between *Synj1*^{+/+} and *Synj1*^{+/-} MB neurons at the soma (**B**) and at the axons (**D**). $N = 1151/1108$ (*Synj1*^{+/+}/*Synj1*^{+/-}) puncta for soma analysis. $N = 432/579$ (*Synj1*^{+/+}/*Synj1*^{+/-}) puncta for axon analysis. **E, F**, Cathepsin-B activity analysis using the Magic Red dye. **E**, Representative images showing the Magic Red signal from live cell imaging and the MAP2 signal from *post hoc* staining for *Synj1*^{+/+} and *Synj1*^{+/-} MB neurons. **F**, Quantification of the intensity of Magic Red signal between *Synj1*^{+/+} and *Synj1*^{+/-} MB neurons. $N = 78/159$ (*Synj1*^{+/+}/*Synj1*^{+/-}) neurons. Extended Data Figure 3-1 shows that Synj1 deficiency does not alter the Cathepsin B expression in MB neurons. **G, H**, Analysis of endolysosomal protease activity using BSA-DQ. **G**, Representative images. **H**, Quantification results, $N = 90/111$ (*Synj1*^{+/+}/*Synj1*^{+/-}) neurons. The p values for **B** and **D** are from two-sample Kolmogorov–Smirnov test, and those for **F** and **H** are from Student’s t test. Scale bar in all images: 10 μm.

To investigate acidity, we expressed a ratiometric lysosomal pH biosensor, Fluorescence Indicator REporting pH in Lysosomes (FIRE-pHLy, hereafter called pHLy; Chin et al., 2021). PHLy was engineered by tagging a cyan pH-sensitive fluorescent protein variant, mTFP1 ($pK_a = 4.3$), to the luminal portion of the human LAMP1 cDNA and an mCherry to the cytosolic side. It was shown that the pHLy biosensor is targeted to express on LAMP1 vesicles and reports luminal pH between 3.5 and 6 (Chin et al., 2021). Surprisingly, our live cell analysis found that endolysosomal acidity was increased in Synj1-deficient neurons both at the soma (Fig. 3A,B) and at the axon (Fig. 3C,D). The hyperacidified endolysosomes may result in elevated enzymatic activity in Synj1-deficient neurons. To test this, we performed two live cell staining assays to analyze cathepsin B activity and general protease activity. For cathepsin B analysis, we incubated the cultures with Magic Red, a substrate of the lysosomal cathepsin-B enzyme that fluoresces red on cleavage by active cathepsin enzymes. As expected, we found that the MR fluorescence was increased in *Synj1*^{+/-} neurons (Fig. 3E,F) without changes in the cathepsin B expression level (Extended Data Fig. 3-1), indicating enhanced enzymatic activity. To further verify a general increase in endolysosomal protease activity, we next conducted a DQ-red BSA (DQ-BSA) assay. Like Magic Red, DQ-BSA is a fluorogenic substrate

that fluoresces on hydrolysis by proteases. Consistently, we found increased DQ-BSA fluorescence in *Synj1*^{+/-} neurons (Fig. 3G,H), suggesting an increase in overall protease activity.

Endolysosome defect is associated with Synj1’s SAC1 activity

To further understand how the two enzymatic domains of Synj1 regulates endolysosomes, we expressed wild-type (WT) and mutant human SYNJ1 (SJ1) cDNAs in Neuro 2a (N2a) cells. Among all mutants we examined, SJ1 R258Q and SJ1 R839C were previously identified in Parkinsonism patients (Krebs et al., 2013; Quadri et al., 2013; Taghavi et al., 2018). The R258Q mutation abolishes SAC1 activity, and the R839C mutation reduces both SAC1 and 5′-phosphatase activities (Pan et al., 2020). The SJ1 D769A is not disease linked but abolishes 5′-phosphatase activity (Mani et al., 2007). Overexpressing WT SJ1 led to an increase in LAMP2A immunofluorescence compared with the empty GFP vector expressing cells (Fig. 4A,B). In contrast, the SJ1 R258Q mutant significantly downregulated LAMP2A expression, whereas the SJ1 R839C mutant produced a less significant effect on downregulating LAMP2A (Fig. 4A,B). Interestingly, the SJ1 D769A mutation did not alter the LAMP2A expression, suggesting that

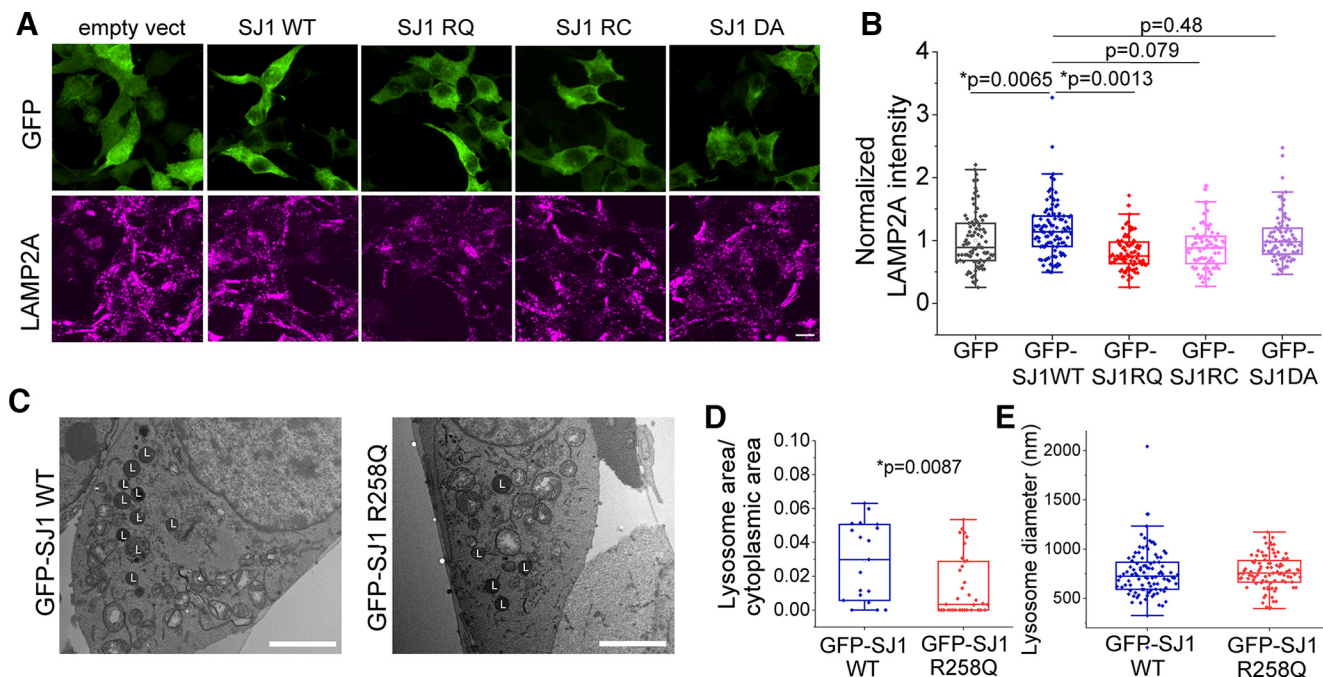


Figure 4. The SAC domain of Synj1 regulates endolysosomal abundance in N2a cells. **A, B**, Immunofluorescence analysis of LAMP2A in N2a cells transfected with GFP, GFP-hSYNJ1 WT, GFP-hSYNJ1 R258Q, GFP-hSYNJ1 R839C, and GFP-hSYNJ1 D769A. **A**, Representative images. **B**, Quantification results, $N = 91/104/88/80/84$ (GFP/GFP-SJ1WT/GFP-SJ1RQ/GFP-SJ1RC/GFP-SJ1DA) cells. p values are from Tukey's *post hoc* following one-way ANOVA. **C–E**, EM analysis of lysosome in N2a cells transfected with GFP-SJ1 WT and GFP-SJ1 R258Q. **C**, Representative EM images. L, lysosome. **D**, Quantification of the ratio of lysosome occupied area to cytoplasmic area in EM images for the two groups, $N = 19/35$ (*Synj1*^{+/+}/*Synj1*^{+/-}) ROIs. **E**, Quantification of lysosome diameter in the EM images of the two groups, $N = 97/95$ (*Synj1*^{+/+}/*Synj1*^{+/-}) lysosomes. The p value is from Student's *t* test. Scale bars: 10 μm (**A**) and 1 μm (**C**).

SAC1 rather than 5'-phosphatase activity is involved in LAMP2A regulation. We further performed electron microscopy (EM) analysis for SJ1 R258Q-expressing cells sorted by a fluorescence-activated cell sorting (FACS) system (Fig. 4C). Compared with those expressing WT SJ1, we found the lysosome density was decreased in N2a cells transfected with SJ1 R258Q (Fig. 4D), while the lysosome size was not affected (Fig. 4E). These results, taken together, suggested that the Synj1's SAC1 domain is important for regulating lysosome quantity.

Synj1 deficiency impairs α -syn A53T degradation in the axon

To determine the physiological impact of endolysosomal change in *Synj1*^{+/-} neurons, we sought to investigate chaperone-mediated autophagy (CMA), which is mediated directly by LAMP2A. We hypothesized that the reduced LAMP2A would result in defective clearance of CMA substrates, such as the α -syn (Cuervo et al., 2004). We first assessed the degradation efficiency of the WT α -syn by tagging it to mEos3.2, a photo-switchable fluorescent protein. Upon UV irradiation, the green fluorescent α -syn-mEos3.2 will switch to a red-shifted protein (Zhang et al., 2012; Fig. 5A), allowing tracking of protein degradation without interference from nascent protein synthesis. In both cell bodies and axons of *Synj1*^{+/-} neurons, we did not observe significant defects in α -syn-mEos3.2 protein

degradation in a 16-hour chase experiment (Fig. 5B,C). More surprisingly, a 16-hour incubation of 2 μM paraquat, a widely studied PD-inducing herbicide and oxidant, was also not able to produce any defect in clearing WT α -syn in the *Synj1*^{+/-} MB neurons (Extended Data Fig. 5-1), although a toxic effect on degradational capacity was observed comparing to naive conditions (Fig. 5B,C; Extended Data Fig. 5-1). We further investigated the degradation efficiency of α -syn A53T, a prevalent mutation of α -syn found in familial PD patients (Polymeropoulos et al., 1997). We found that cell bodies of *Synj1*^{+/-} neurons could clear the UV converted α -syn A53T-mEos3.2 as effectively as the *Synj1*^{+/+} neurons (Fig. 5D,E). However, the axons of *Synj1*^{+/-} neurons exhibited a significant impairment (Fig. 5F,G), suggesting specific vulnerability in Synj1-deficient axons to protein stress. Taken together, our results suggest an impaired endolysosomal system in Synj1-deficient midbrain neurons, which could result in a specific vulnerability in axonal protein degradation.

Discussion

In this study, we performed a comprehensive analysis of cellular degradation systems in cultured *Synj1*^{+/-} MB neurons. We found that baseline autophagy flux revealed by GFP-LC3 is largely unaltered in the neuronal cell body. However, we show, for the first time, that Synj1 regulates endolysosomal biology. The LAMP1 vesicle abundance is reduced in the soma and axons of *Synj1*^{+/-} MB neurons,

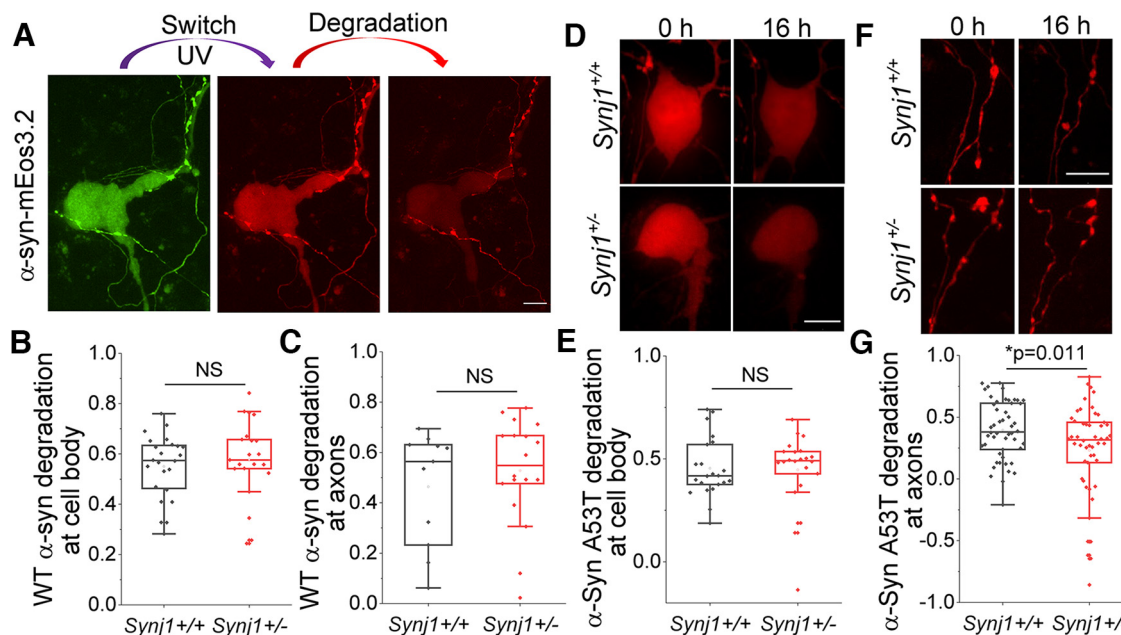


Figure 5. Synj1 deficiency impairs the degradation of α -Syn A53T in axons of cultured MB neurons. **A–C**, The α -syn WT-mEos3.2 degradation analysis at soma and axons in cultured MB neurons. **A**, Representative images. **B**, Quantification for the fraction of degradation of α -syn WT-mEos3.2 at soma within 16 hours. $N=24/21$ ($Synj1^{+/+}/Synj1^{+/-}$) neurons. NS: $p > 0.05$ (two-tailed Student's t test). **C**, Quantification for the fraction of degradation of α -syn WT-mEos3.2 at axons, $N=11/18$ ($Synj1^{+/+}/Synj1^{+/-}$) axons. NS: $p > 0.05$ (two-tailed Student's t test). Extended Data Figure 5-1 shows that paraquat incubation induces similar impairments in the degradation of α -syn WT-mEos3.2 in $Synj1^{+/+}$ and $Synj1^{+/-}$ neurons. **D–G**, The α -syn A53T-mEos3.2 16-hour degradation analysis at soma and axons in cultured MB neurons. **D**, Representative images of soma. **E**, Quantification for the fraction of degradation of α -syn A53T-mEos3.2 at soma. $N=22/22$ ($Synj1^{+/+}/Synj1^{+/-}$) neurons. NS: $p > 0.05$ (two-tailed Student's t test). **F**, Representative images of axon. **G**, Quantification for the fraction of degradation of α -syn-mEos3.2 A53T at axon, $N=50/50$ ($Synj1^{+/+}/Synj1^{+/-}$) axons. The p value is from two-tailed Student's t test. Scale bar in all images: 10 μ m.

along with a general decrease in lysosomal-associated membrane proteins, including LAMP1, LAMP2, and LAMP2A. We show that the SAC1 activity of Synj1 is more important relative to the 5'-phosphatase activity for maintaining endolysosomal abundance. Interestingly, the acidity and enzymatic activity of the endolysosomal compartments are enhanced in $Synj1^{+/-}$ MB neurons, which may be a direct result of Synj1 deficiency or representative of compensatory changes. We further examined the impact of Synj1 deficiency on cellular degradation by chasing the fluorescence decrease of exogenously expressed α -syn WT and A53T mutant proteins. We found that the degradation of WT α -syn, which under normal conditions relies on LAMP2A-mediated CMA (Cuervo et al., 2004; Kuo et al., 2022) is normal in the cell body and axons of $Synj1^{+/-}$ MB neurons, suggesting adequate compensation. However, the A53T α -syn exhibited impaired degradation in the axons of $Synj1^{+/-}$ MB neurons, suggesting an axon-specific vulnerability in removing stress proteins.

A series of recent investigation suggested a regulatory role of Synj1 in various stages of autophagy. Contradictory to findings from the mouse astrocyte study that showed enhanced LC3 puncta in $Synj1^{+/-}$ and $-/-$ backgrounds (Pan et al., 2021), and those from the *Drosophila* neuromuscular junction (NMJ) study that showed impaired LC3 puncta formation in the *Synj* RQ mutation knock-in background (Vanhouwaert et al., 2017), our study of the mouse $Synj1^{+/-}$ MB neurons suggested that Synj1 is not essential for maintaining basal level GFP-LC3 puncta and

clearance at the neuronal cell body. This lack of change is likely because of lower metabolic demands at the neuronal soma at baseline compared astrocytes, and less membrane trafficking at the neuronal soma compared with an active synapse (i.e., NMJ). One limitation of the cell culture work is that it is difficult to reveal changes associated with age-related stress. A previous *in vivo* study in aged *Synj1* haploinsufficient ($Synj1^{+/-}$) mice demonstrated an accumulation of the autophagy substrate p62 in the midbrain DA neuron cell bodies (Pan et al., 2020), suggesting that the unaltered LC3 clearance we observed in culture was likely because of compensation at a stress-free condition.

Synj1 has two phosphatase domains: the SAC1 domain enzyme that hydrolyzes PI(3)P, PI(4)P, and PI(3,5)P₂; and the 5'-phosphatase domain enzyme that primarily hydrolyzes PI(4,5)P₂. Different phosphoinositides are enriched in different subcellular compartments, acting as organizers of membrane organelles and participating in cellular signaling (Posor et al., 2022). For instance, studies have shown that despite the low abundance of PI(3,5)P₂ in cells, it is implicated in autophagosome maturation (Vanhouwaert et al., 2017) and important for lysosome formation and ion homeostasis (McCartney et al., 2014; Hasegawa et al., 2017; Ebner et al., 2019). Synj1 deficiency could lead to an accumulation of PI(3,5)P₂ to interfere with lysosomal function. In our study we showed that LAMP2A was decreased in $Synj1^{+/-}$ neurons and Synj1 R258Q-expressing N2a cells, but not in Synj1 D769A or Synj1 R839C expressing cells. This

suggests an involvement of SAC1 activity and, also, that the PI(3,5)P₂ may negatively regulate endolysosomal protein expression. Indeed, PI(3,5)P₂ is broadly involved in regulating lysosomal protein expression. It was found that PI(3,5)P₂ can activate mTORC1 through direct binding to the mTORC1 subunit Raptor in yeast, which phosphorylates TFEB and, thereby, inhibits lysosomal gene expression (Bridges et al., 2012; Jin et al., 2014). Whether mTORC1 signaling is activated in *Synj1*^{+/-} MB neurons to downregulate LAMP protein expression awaits further analysis.

Previous studies in yeast also shown that PI(3,5)P₂ could directly bind to Vph1, a subunit of V-ATPase, to regulate V-ATPase assembly and proton pumping activity both *in vitro* and *in vivo* (Li et al., 2014; Banerjee et al., 2019). This is in line with our finding that endolysosomal acidity is significantly higher in *Synj1*^{+/-} MB neurons compared with littermate WT neurons. Interestingly, while endolysosomes are much more acidic in *Synj1*^{+/-} neurons than in *Synj1*^{+/+} neurons, the acidity of the mKeima structures was not different. This could be attributed to the lack of power in the mKeima analysis, but it is also plausible that autophagosome-lysosome fusion is impaired in *Synj1*^{+/-} MB neurons. For example, it was shown that PI(4,5)P₂ not only mediates clathrin-AP2 coats assembly at the plasma membrane but also induces tubular protolysosome budding from tubular intermediates of autolysosomes (Rong et al., 2012), and participates in autophagosome and lysosome fusion (Posor et al., 2022). Whether the increased PI(4,5)P₂ in *Synj1*^{+/-} MB neurons (Pan et al., 2020) plays a role in disrupting the fusion between autophagosomes and lysosomes requires further investigation.

Despite finding multiple endolysosomal abnormalities in *Synj1*^{+/-} MB neurons, we did not observe alterations in WT α -syn clearance at baseline or under paraquat stressed conditions. These data were striking as an accumulation of total and phosphorylated α -syn was reported in aged *Synj1*^{+/-} male mice across multiple brain regions including the MB and striatum (Pan et al., 2020). Our data obtained from cultured MB neurons of mixed sex suggest several possibilities: (1) the degradation capacity of the MB neurons declines during aging, which is not captured in a culture system and is likely independent of oxidative stress; (2) the accumulation of α -syn proteins is a result of impaired glial function as opposed to neuronal degradation (Kam et al., 2020; Scheiblich et al., 2021); (3) the accumulation of α -syn proteins is a male-specific defect, which was diluted in the mixed sex culture. Interestingly, the degradation of the mutant protein, α -syn A53T, was significantly impaired in the axons of *Synj1*^{+/-} neurons. Studies have shown that mutant α -syn exhibit impaired uptake by LAMP2A via the CMA pathway (Cuervo et al., 2004). Therefore, the impaired A53T α -syn degradation in *Synj1*^{+/-} axons is likely because of mechanisms other than CMA, such as defective axonal autophagy, which was not extensively investigated in the current study because of technical limitations but supported by findings from invertebrate models of *Synj* deletion (Vanhouwaert et al., 2017; Yang et al., 2022). In summary, our data were

largely consistent with findings from previous *in vivo* studies (Pan et al., 2020) and astrocyte cultures (Pan et al., 2021), which found that *Synj1* haploinsufficient neurons and glia become more vulnerable during aging with accumulating cellular stress. We now suggest that axons of *Synj1*^{+/-} neurons are more vulnerable than cell bodies, supporting the dying back theory in *Synj1* deficiency associated neurodegeneration (Bernheimer et al., 1973) and such axonal vulnerability could contribute in part to loss of dopaminergic innervation in aged *Synj1*-deficient brains (Pan et al., 2020).

References

- Banerjee S, Clapp K, Tarsio M, Kane PM (2019) Interaction of the late endo-lysosomal lipid PI(3,5)P₂ with the Vph1 isoform of yeast V-ATPase increases its activity and cellular stress tolerance. *J Biol Chem* 294:9161–9171.
- Bernheimer H, Birkmayer W, Hornykiewicz O, Jellinger K, Seitelberger F (1973) Brain dopamine and the syndromes of Parkinson and Huntington. Clinical, morphological and neurochemical correlations. *J Neurol Sci* 20:415–455.
- Bridges D, Ma JT, Park S, Inoki K, Weisman LS, Saitel AR (2012) Phosphatidylinositol 3,5-bisphosphate plays a role in the activation and subcellular localization of mechanistic target of rapamycin 1. *Mol Biol Cell* 23:2955–2962.
- Cheng XT, Xie YX, Zhou B, Huang N, Farfel-Becker T, Sheng ZH (2018a) Revisiting LAMP1 as a marker for degradative autophagy-lysosomal organelles in the nervous system. *Autophagy* 14:1472–1474.
- Cheng XT, Xie YX, Zhou B, Huang N, Farfel-Becker T, Sheng ZH (2018b) Characterization of LAMP1-labeled nondegradative lysosomal and endocytic compartments in neurons. *J Cell Biol* 217:3127–3139.
- Chin MY, Patwardhan AR, Ang KH, Wang AL, Alquezar C, Welch M, Nguyen PT, Grabe M, Molofsky AV, Arkin MR, Kao AW (2021) Genetically encoded, pH-sensitive mTFP1 biosensor for probing lysosomal pH. *ACS Sens* 6:2168–2180.
- Cremona O, Di Paolo G, Wenk MR, Lüthi A, Kim WT, Takei K, Daniell L, Nemoto Y, Shears SB, Flavell RA, McCormick DA, De Camilli P (1999) Essential role of phosphoinositide metabolism in synaptic vesicle recycling. *Cell* 99:179–188.
- Cuervo AM, Dice JF (1996) A receptor for the selective uptake and degradation of proteins by lysosomes. *Science* 273:501–503.
- Cuervo AM, Stefanis L, Fredenburg R, Lansbury PT, Sulzer D (2004) Impaired degradation of mutant alpha-synuclein by chaperone-mediated autophagy. *Science* 305:1292–1295.
- Ebner M, Koch PA, Haucke V (2019) Phosphoinositides in the control of lysosome function and homeostasis. *Biochem Soc Trans* 47:1173–1185.
- Fleming A, Bourdenx M, Fujimaki M, Karabiyik C, Krause GJ, Lopez A, Martín-Segura A, Puri C, Scervo A, Skidmore J, Son SM, Stamatakou E, Wrobel L, Zhu Y, Cuervo AM, Rubinsztein DC (2022) The different autophagy degradation pathways and neurodegeneration. *Neuron* 110:935–966.
- George AA, Hayden S, Holzhausen LC, Ma EY, Suzuki SC, Brockerhoff SE (2014) Synaptojanin 1 is required for endolysosomal trafficking of synaptic proteins in cone photoreceptor inner segments. *PLoS One* 9:e84394.
- George AA, Hayden S, Stanton GR, Brockerhoff SE (2016) Arf6 and the 5'phosphatase of synaptojanin 1 regulate autophagy in cone photoreceptors. *Bioessays* 38 [Suppl 1]:S119–S135.
- Guo S, Stolz LE, Lemrow SM, York JD (1999) SAC1-like domains of yeast SAC1, INP52, and INP53 and of human synaptojanin encode polyphosphoinositide phosphatases. *J Biol Chem* 274:12990–12995.

- Hasegawa J, Strunk BS, Weisman LS (2017) PI5P and PI(3,5)P₂: minor, but essential phosphoinositides. *Cell Struct Funct* 42:49–60.
- Henderson MX, Henrich MT, Geibl FF, Oertel WH, Brundin P, Surmeier DJ (2022) The roles of connectivity and neuronal phenotype in determining the pattern of α -synuclein pathology in Parkinson's disease. *Neurobiol Dis* 168:105687.
- Jin N, Mao K, Jin Y, Tevzadze G, Kauffman EJ, Park S, Bridges D, Loewth R, Saltiel AR, Klionsky DJ, Weisman LS (2014) Roles for PI(3,5)P₂ in nutrient sensing through TORC1. *Mol Biol Cell* 25:1171–1185.
- Kam TI, Hinkle JT, Dawson TM, Dawson VL (2020) Microglia and astrocyte dysfunction in Parkinson's disease. *Neurobiol Dis* 144:105028.
- Katayama H, Kogure T, Mizushima N, Yoshimori T, Miyawaki A (2011) A sensitive and quantitative technique for detecting autophagic events based on lysosomal delivery. *Chem Biol* 18:1042–1052.
- Kaushik S, Cuervo AM (2018) The coming of age of chaperone-mediated autophagy. *Nat Rev Mol Cell Biol* 19:365–381.
- Kirola L, Behari M, Shishir C, Thelma BK (2016) Identification of a novel homozygous mutation Arg459Pro in SYNJ1 gene of an Indian family with autosomal recessive juvenile Parkinsonism. *Parkinsonism Relat Disord* 31:124–128.
- Klionsky DJ (2007) Autophagy: from phenomenology to molecular understanding in less than a decade. *Nat Rev Mol Cell Biol* 8:931–937.
- Kon M, Cuervo AM (2010) Chaperone-mediated autophagy in health and disease. *FEBS Lett* 584:1399–1404.
- Krebs CE, Karkheiran S, Powell JC, Cao M, Makarov V, Darvish H, Di Paolo G, Walker RH, Shahidi GA, Buxbaum JD, De Camilli P, Yue Z, Paisán-Ruiz C (2013) The Sac1 domain of SYNJ1 identified mutated in a family with early-onset progressive Parkinsonism with generalized seizures. *Hum Mutat* 34:1200–1207.
- Kuo SH, et al. (2022) Mutant glucocerebrosidase impairs α -synuclein degradation by blockade of chaperone-mediated autophagy. *Sci Adv* 8:eabm6393.
- Li SC, Diakov TT, Xu T, Tarsio M, Zhu W, Couoh-Cardel S, Weisman LS, Kane PM (2014) The signaling lipid PI(3,5)P₂ stabilizes V₁-V(o) sector interactions and activates the V-ATPase. *Mol Biol Cell* 25:1251–1262.
- Mani M, Lee SY, Lucast L, Cremona O, Di Paolo G, De Camilli P, Ryan TA (2007) The dual phosphatase activity of synaptojanin1 is required for both efficient synaptic vesicle endocytosis and reavailability at nerve terminals. *Neuron* 56:1004–1018.
- McCartney AJ, Zhang Y, Weisman LS (2014) Phosphatidylinositol 3,5-bisphosphate: low abundance, high significance. *Bioessays* 36:52–64.
- McPherson PS, Garcia EP, Slepnev VI, David C, Zhang X, Grabs D, Sossin WS, Bauerfeind R, Nemoto Y, De Camilli P (1996) A presynaptic inositol-5-phosphatase. *Nature* 379:353–357.
- Neumann S, Chassefeyre R, Campbell GE, Encalada SE (2017) KymoAnalyzer: a software tool for the quantitative analysis of intracellular transport in neurons. *Traffic* 18:71–88.
- Nixon RA (2013) The role of autophagy in neurodegenerative disease. *Nat Med* 19:983–997.
- Oliveira LMA, Gasser T, Edwards R, Zweckstetter M, Melki R, Stefanis L, Lashuel HA, Sulzer D, Vekrellis K, Halliday GM, Tomlinson JJ, Schlossmacher M, Jensen PH, Schulze-Hentrich J, Riess O, Hirst WD, El-Agnaf O, Mollenhauer B, Lansbury P, Outeiro TF (2021) Alpha-synuclein research: defining strategic moves in the battle against Parkinson's disease. *NPJ Parkinsons Dis* 7:65.
- Pan PY, Li X, Wang J, Powell J, Wang Q, Zhang Y, Chen Z, Wicinski B, Hof P, Ryan TA, Yue Z (2017) Parkinson's disease-associated LRRK2 hyperactive kinase mutant disrupts synaptic vesicle trafficking in ventral midbrain neurons. *J Neurosci* 37:11366–11376.
- Pan PY, Sheehan P, Wang Q, Zhu X, Zhang Y, Choi I, Li X, Saenz J, Zhu J, Wang J, El Gaamouch F, Zhu L, Cai D, Yue Z (2020) Synj1 haploinsufficiency causes dopamine neuron vulnerability and alpha-synuclein accumulation in mice. *Hum Mol Genet* 29:2300–2312.
- Pan PY, Zhu J, Rizvi A, Zhu X, Tanaka H, Dreyfus CF (2021) Synaptojanin1 deficiency upregulates basal autophagosome formation in astrocytes. *J Biol Chem* 297:100873.
- Pirruccello M, De Camilli P (2012) Inositol 5-phosphatases: insights from the Lowe syndrome protein OCRL. *Trends Biochem Sci* 37:134–143.
- Polymeropoulos MH, Lavedan C, Leroy E, Ide SE, Dehejia A, Dutra A, Pike B, Root H, Rubenstein J, Boyer R, Stenroos ES, Chandrasekharappa S, Athanassiadou A, Papapetropoulos T, Johnson WG, Lazzarini AM, Duvoisin RC, Di Iorio G, Golbe LI, Nussbaum RL (1997) Mutation in the alpha-synuclein gene identified in families with Parkinson's disease. *Science* 276:2045–2047.
- Posor Y, Jang W, Haucke V (2022) Phosphoinositides as membrane organizers. *Nat Rev Mol Cell Biol* 23:797–816.
- Quadri M, et al. (2013) Mutation in the SYNJ1 gene associated with autosomal recessive, early-onset Parkinsonism. *Hum Mutat* 34:1208–1215.
- Robak LA, Jansen IE, van Rooij J, Uitterlinden AG, Kraaij R, Jankovic J; International Parkinson's Disease Genomics Consortium (IPDGC); Heutink P, Shulman JM (2017) Excessive burden of lysosomal storage disorder gene variants in Parkinson's disease. *Brain* 140:3191–3203.
- Rong Y, Liu M, Ma L, Du W, Zhang H, Tian Y, Cao Z, Li Y, Ren H, Zhang C, Li L, Chen S, Xi J, Yu L (2012) Clathrin and phosphatidylinositol-4,5-bisphosphate regulate autophagic lysosome reformation. *Nat Cell Biol* 14:924–934.
- Scheiblich H, Dansokho C, Mercan D, Schmidt SV, Bousset L, Wischhof L, Eikens F, Odanic A, Spitzer J, Griep A, Schwartz S, Bano D, Latz E, Melki R, Heneka MT (2021) Microglia jointly degrade fibrillar alpha-synuclein cargo by distribution through tunneling nanotubes. *Cell* 184:5089–5106.e21.
- Surmeier DJ, Obeso JA, Halliday GM (2017) Selective neuronal vulnerability in Parkinson disease. *Nat Rev Neurosci* 18:101–113.
- Taghavi S, et al. (2018) A clinical and molecular genetic study of 50 families with autosomal recessive Parkinsonism revealed known and novel gene mutations. *Mol Neurobiol* 55:3477–3489.
- Udayar V, Chen Y, Sidransky E, Jagasia R (2022) Lysosomal dysfunction in neurodegeneration: emerging concepts and methods. *Trends Neurosci* 45:184–199.
- Vanhauwaert R, et al. (2017) The SAC1 domain in synaptojanin is required for autophagosome maturation at presynaptic terminals. *EMBO J* 36:1392–1411.
- Vázquez-Vélez GE, Zoghbi HY (2021) Parkinson's disease genetics and pathophysiology. *Annu Rev Neurosci* 44:87–108.
- Verstreken P, Kjaerulf O, Lloyd TE, Atkinson R, Zhou Y, Meinertzhagen IA, Bellen HJ (2002) Endophilin mutations block clathrin-mediated endocytosis but not neurotransmitter release. *Cell* 109:101–112.
- Verstreken P, Koh TW, Schulze KL, Zhai RG, Hiesinger PR, Zhou Y, Mehta SQ, Cao Y, Roos J, Bellen HJ (2003) Synaptojanin is recruited by endophilin to promote synaptic vesicle uncoating. *Neuron* 40:733–748.
- Yang S, Park D, Manning L, Hill SE, Cao M, Xuan Z, Gonzalez I, Dong Y, Clark B, Shao L, Okeke I, Almoril-Porras A, Bai J, De Camilli P, Colon-Ramos DA (2022) Presynaptic autophagy is coupled to the synaptic vesicle cycle via ATG-9. *Neuron* 110:824–840.e10.
- Zhang M, Chang H, Zhang Y, Yu J, Wu L, Ji W, Chen J, Liu B, Lu J, Liu Y, Zhang J, Xu P, Xu T (2012) Rational design of true monomeric and bright photoactivatable fluorescent proteins. *Nat Methods* 9:727–729.
- Zhong S, Hsu F, Stefan CJ, Wu X, Patel A, Cosgrove MS, Mao Y (2012) Allosteric activation of the phosphoinositide phosphatase Sac1 by anionic phospholipids. *Biochemistry* 51:3170–3177.
- Zhu X, Li M, Xu X, Zhang R, Zhang X, Ma Z, Lu J, Xu T, Hou J, Song E (2018) hTAC internalizes via both clathrin-dependent and clathrin-independent endocytosis in mammalian cells. *Protein Cell* 9:896–901.